

Article

# Design, Synthesis, and Evaluation of *B*-(Trifluoromethyl)phenyl Phosphine–Borane Derivatives as Novel Progesterone Receptor Antagonists

Yu Miyajima , Kotaro Ochiai and Shinya Fujii \*

Institute of Biomaterials and Bioengineering, Tokyo Medical and Dental University, 2-3-10 Kanda-Surugadai, Chiyoda-ku, Tokyo 101-0062, Japan

\* Correspondence: fujiis.chem@tmd.ac.jp

**Abstract:** We previously revealed that phosphine–boranes can function as molecular frameworks for biofunctional molecules. In the present study, we exploited the diversity of available phosphines to design and synthesize a series of *B*-(trifluoromethyl)phenyl phosphine–borane derivatives as novel progesterone receptor (PR) antagonists. We revealed that the synthesized phosphine–borane derivatives exhibited  $\text{Log}P$  values in a predictable manner and that the P–H group in the phosphine–borane was almost nonpolar. Among the synthesized phosphine–boranes, which exhibited PR antagonistic activity, *B*-(4-trifluoromethyl)phenyl tricyclopropylphosphine–borane was the most potent with an  $\text{IC}_{50}$  value of 0.54  $\mu\text{M}$ . A docking simulation indicated that the tricyclopropylphosphine moiety plays an important role in ligand–receptor interactions. These results support the idea that phosphine–boranes are versatile structural options in drug discovery, and the developed compounds are promising lead compounds for further structural development of next-generation PR antagonists.

**Keywords:** phosphorus; phosphine–borane; hydrophobicity; progesterone receptor; antagonist; structural optimization



**Citation:** Miyajima, Y.; Ochiai, K.; Fujii, S. Design, Synthesis, and Evaluation of *B*-(Trifluoromethyl)-phenyl Phosphine–Borane Derivatives as Novel Progesterone Receptor Antagonists. *Molecules* **2024**, *29*, 1587. <https://doi.org/10.3390/molecules29071587>

Academic Editors: György Keglevich and Dobromir Enchev

Received: 16 February 2024

Revised: 26 March 2024

Accepted: 27 March 2024

Published: 2 April 2024



**Copyright:** © 2024 by the authors. Licensee MDPI, Basel, Switzerland. This article is an open access article distributed under the terms and conditions of the Creative Commons Attribution (CC BY) license (<https://creativecommons.org/licenses/by/4.0/>).

## 1. Introduction

Phosphine–boranes are complexes of phosphines and boranes bearing P–B bonds [1–3]. Owing to the stability of the P–B bond in the adducts, phosphine–boranes are utilized as synthetic intermediates of phosphines: the borane moiety functions as a protective group for the oxidation-susceptible lone pair of trivalent phosphorus [4–6]. P–B adducts have also been investigated for biomedical applications such as boranophosphate-type nucleic acids (1), in which the P=O double bond of the phosphate moiety is replaced by a P–B bond [7,8]. Levin et al. developed phosphine–boranes bearing a P–BH<sub>3</sub> moiety, such as compound 2, as neuroprotective agents (Figure 1) [9,10]. From a structural arrangement perspective, the P–B substructures in phosphine–boranes can be regarded as isosteric with alkanes because of their tetrahedral sp<sup>3</sup>–sp<sup>3</sup> character. Based on this consideration, we recently developed phosphine–borane-containing estrogen receptor (ER) modulators such as 3 and 4 [11,12]. Subsequently, we had revealed that the P–BH<sub>2</sub>–Ph moiety as well as P–BH<sub>3</sub> moieties are useful structural options for the development of biologically active compounds, particularly for the optimization of hydrophobic substructures by controlling the hydrophobicity of the compounds. In the current study, to investigate the general usefulness of phosphine–boranes for other biological targets, we aimed to investigate the development of novel progesterone receptor (PR) antagonists based on a phosphine–borane framework.

The progesterone receptor (PR) is a member of the nuclear receptor superfamily of ligand-dependent transcription factors and plays important roles in multiple physiological processes including the female reproductive system, such as in uterine cell proliferation and differentiation, ovulation cycle, and mammary gland growth and differentiation [13,14]. The PR is regulated by the endogenous steroidal agonist progesterone (P4, 5, Figure 2).

Various steroidal PR agonists have been developed and are clinically used for the treatment of gynecological disorders, contraception, and hormone replacement therapy [15,16]. In addition to PR agonists, PR antagonists have attracted considerable attention as drug candidates. Although the representative, approved PR antagonist mifepristone (**6**) is currently in limited clinical use as an abortifacient, ulipristal acetate (**7**) is used not only as a contraceptive agent but also as a treatment for uterine fibroids [17–20]. Studies using PR antagonists, such as **6** and the investigational drug onapristone (**8**), indicated that PR antagonists might be effective not only for contraception and uterine fibroids but also for the treatment of endometriosis, breast cancer, ovarian cancer, uterine cancer, and some psychiatric disorders [21–27]. In contrast, all PR antagonists used clinically, including **6** and **7**, are steroidal compounds. Therefore, the development of nonsteroidal PR antagonists is preferred to avoid side effects related to target selectivity and metabolic pathways. Indeed, a few steroidal PR antagonists, including **6**, demonstrate potent activities against other steroid receptors, such as the glucocorticoid receptor (GR) [28–30]. Thus, various nonsteroidal PR antagonists such as **10–13** [31–37] have been synthesized based on the structure of the nonsteroidal PR agonist tanaproget (**9**) [38]. These compounds have a common cyanoaryl moiety as the pharmacophore motif, and minor structural modifications of PR ligands bearing this motif can cause agonist/antagonist activity switching [32,33,38,39]. We have been investigating the development of new-generation PR antagonists and have reported that PR antagonists such as **14** and **15** are structurally distinct from conventional nonsteroidal PR antagonists (Figure 2) [40,41]. Regarding PR antagonists and ligands of other nuclear receptors, hydrophobic interactions are essential for ligand activity. Thus, we hypothesized that the application of the phosphine–borane moiety is advantageous for the structural development of the hydrophobic moiety in PR antagonists. Consequently, we developed novel phosphine–borane framework-based PR antagonists.

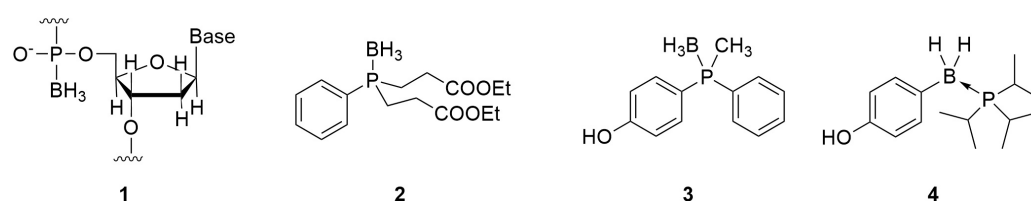


Figure 1. Examples of P–B bond-containing biofunctional molecules.

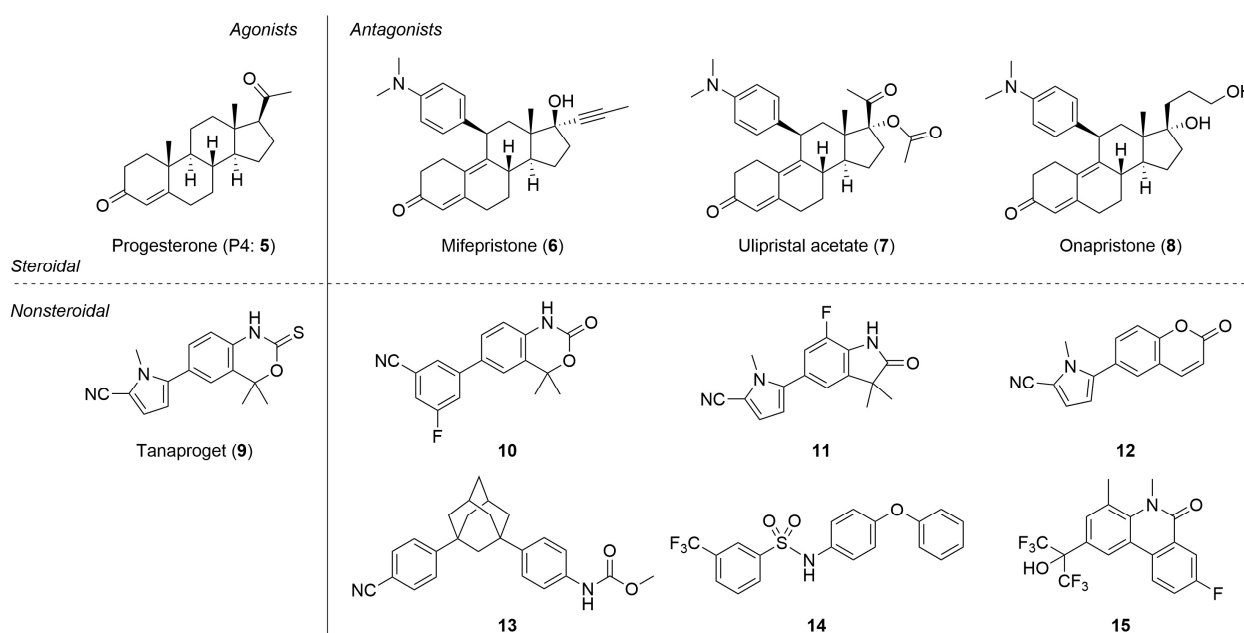
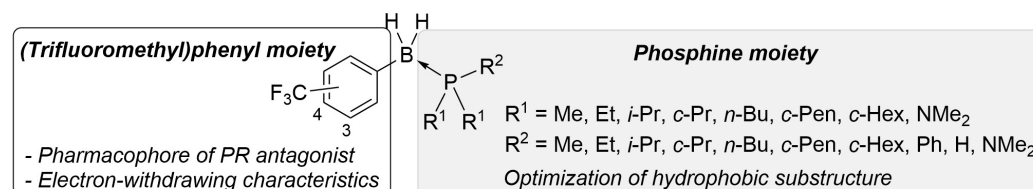


Figure 2. Structures of the endogenous PR agonist **5** and representative synthetic PR agonists and antagonists.

## 2. Results and Discussion

### 2.1. Molecular Design

To develop a novel nonsteroidal PR antagonist, we adopted the (trifluoromethyl)phenyl group as the key structural motif, which has been found to function as a pharmacophore for PR antagonists such as **14**. Our recent results indicated that the electronic profile of the *B*-substituents of phosphine–boranes partly influences the stability of the compounds, and an increase in the electrophilicity of the boron atom can increase the stability of the phosphine–borane adducts [12]. Thus, the introduction of an electron-withdrawing trifluoromethyl group onto the *B*-phenyl moiety is a reasonable approach for designing novel biologically active phosphine–borane derivatives. In addition, phosphine–borane frameworks are less hydrophobic than the corresponding carbon-based frameworks [11,12]; therefore, the introduction of a highly hydrophobic trifluoromethyl group on the phosphine–borane framework can provide appropriate hydrophobicity to the compounds. Regarding the phosphine moiety, various phosphines with diverse shapes and bulkiness are available because of their utility as phosphine ligands in catalysts. We assumed that the structural diversity of phosphines is particularly useful for the optimization of a hydrophobic motif in PR antagonists. Hence, we designed a series of *B*-(trifluoromethyl)phenyl phosphine–borane derivatives bearing a wide variety of phosphine moieties (Figure 3).



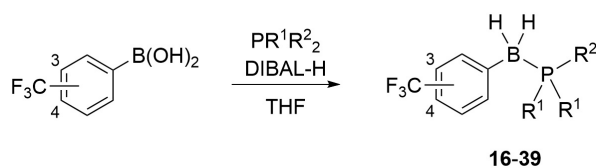
**Figure 3.** Design scheme of the *B*-(trifluoromethyl)phenyl phosphine–borane derivatives as PR antagonists.

### 2.2. Synthesis

The designed *B*-(trifluoromethyl)phenyl phosphine–borane derivatives **16–39** were synthesized from the corresponding phosphines and 3- or 4-(trifluoromethyl)phenyl boronic acid under reductive conditions (Scheme 1) [12,42,43]. Interestingly, we could obtain phosphine–borane derivatives **26** and **38** containing the P–H moiety under normal preparation conditions using an aqueous workup. We also obtained tris(dimethylamino)phosphine–borane derivatives **27** and **39**.

### 2.3. Hydrophobicity

Hydrophobicity is a key determinant of the activity and pharmacokinetics of biologically active compounds, and the octanol–water partition coefficient (*P*) and logarithm value ( $\text{Log}P$ ) are widely used hydrophobicity parameters [44]. The  $\text{Log}P$  values of the synthesized compounds were determined using HPLC [45,46]. Table 1 summarizes the experimentally determined  $\text{Log}P$  values and calculated values. The trimethylphosphine–borane derivatives **16** and **28** exhibited a  $\text{Log}P$  value of 3.65. In our previous study, the corresponding phenol derivative *B*-4-hydroxyphenyl trimethylphosphine–borane exhibited a  $\text{Log}P$  value of 2.44 [12]. The reported substituent constants of hydrophobicity of the  $\text{CF}_3$  and phenolic OH groups were 0.88 and  $-0.67$ , respectively [47], and therefore, the difference between the  $\text{Log}P$  values of trifluoride and the corresponding phenol derivative moderately agreed with the reported difference. From the viewpoint of the phosphine structure, an increase in the number of carbon atoms increased hydrophobicity in a predictable manner. Compounds **26** and **38** bearing a P–H group and two cyclohexyl groups exhibited  $\text{Log}P$  values of 7.28 and 7.34, respectively. These  $\text{Log}P$  values were similar to those of the tri-*n*-butyl derivatives **23** ( $\text{Log}P = 7.34$ ) and **35** ( $\text{Log}P = 7.50$ ) possessing the same number of carbon atoms ( $\text{C}_{12}$ ), indicating that the P–H group in the phosphine–borane derivative was almost nonpolar and did not significantly reduce the hydrophobicity of the compounds.



Cmpd	R <sup>1</sup>	R <sup>2</sup>	Yield	Cmpd	R <sup>1</sup>	R <sup>2</sup>	Yield
16	Me	Me	67%	28	Me	Me	24%
17	Me	Ph	68%	29	Me	Ph	28%
18	Et	Et	26%	30	Et	Et	49%
19	Et	Ph	67%	31	Et	Ph	38%
20	<i>i</i> -Pr	<i>i</i> -Pr	54% <sup>a</sup>	32	<i>i</i> -Pr	<i>i</i> -Pr	13% <sup>a</sup>
21	<i>i</i> -Pr	Ph	25% <sup>a</sup>	33	<i>i</i> -Pr	Ph	18% <sup>a</sup>
22	<i>c</i> -Pr	<i>c</i> -Pr	26% <sup>a</sup>	34	<i>c</i> -Pr	<i>c</i> -Pr	22% <sup>a</sup>
23	<i>n</i> -Bu	<i>n</i> -Bu	66%	35	<i>n</i> -Bu	<i>n</i> -Bu	15%
24	<i>c</i> -Pen	<i>c</i> -Pen	60%	36	<i>c</i> -Pen	<i>c</i> -Pen	32%
25	<i>c</i> -Hex	<i>c</i> -Hex	45%	37	<i>c</i> -Hex	<i>c</i> -Hex	29%
26	<i>c</i> -Hex	H	31%	38	<i>c</i> -Hex	H	37%
27	NMe <sub>2</sub>	NMe <sub>2</sub>	23%	39	NMe <sub>2</sub>	NMe <sub>2</sub>	23%

**Scheme 1.** Synthesis of the designed *B*-(trifluoromethyl)phenyl phosphine–borane derivatives **16–39**.

<sup>a</sup> The yield was calculated in two steps: (1) synthesis of phosphines without purification, (2) reductive P–B bond formation using DIBAL-H.

**Table 1.** Determined Log*P* values and calculated hydrophobicity parameters MLOGP and WLOGP of the synthesized phosphine–borane derivatives **16–39**.

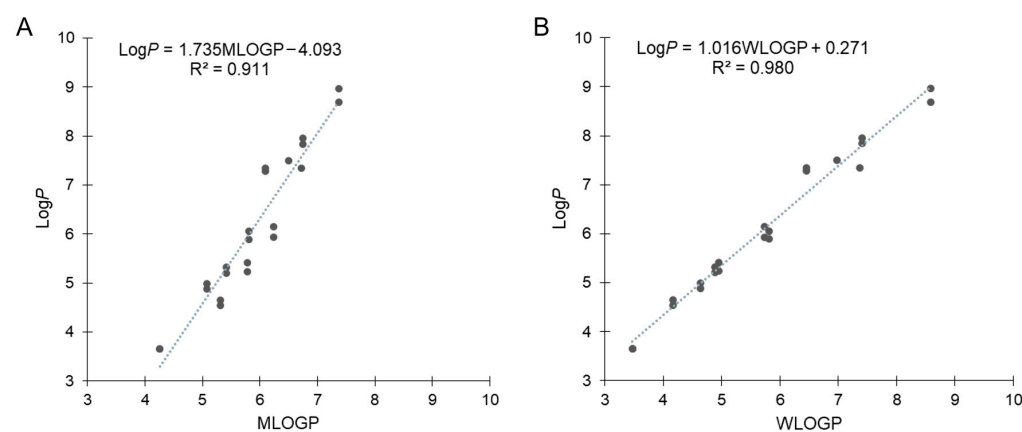
Cmpd	R <sup>1</sup>	R <sup>2</sup>	Log <i>P</i>	MLOGP	Δ(Log <i>P</i> –MLOGP)	WLOGP	Δ(Log <i>P</i> –WLOGP)
16	Me	Me	3.65	4.26	−0.61	3.47	0.18
17	Me	Ph	4.54	5.31	−0.77	4.17	0.37
18	Et	Et	4.88	5.07	−0.19	4.64	0.24
19	Et	Ph	5.24	5.78	−0.54	4.95	0.29
20	<i>i</i> -Pr	<i>i</i> -Pr	5.89	5.81	0.08	5.81	0.08
21	<i>i</i> -Pr	Ph	5.93	6.24	−0.31	5.73	0.20
22	<i>c</i> -Pr	<i>c</i> -Pr	5.21	5.41	−0.20	4.88	0.33
23	<i>n</i> -Bu	<i>n</i> -Bu	7.34 <sup>a</sup>	6.72	0.62	7.37	−0.03
24	<i>c</i> -Pen	<i>c</i> -Pen	7.84 <sup>a</sup>	6.75	1.09	7.41	0.43
25	<i>c</i> -Hex	<i>c</i> -Hex	8.69 <sup>a</sup>	7.37	1.32	8.58	0.11
26	<i>c</i> -Hex	H	7.28 <sup>a</sup>	6.10	1.18	6.45	0.83
27	NMe <sub>2</sub>	NMe <sub>2</sub>	5.39	3.00	2.39	3.01	2.38

Table 1. Cont.

Cmpd	R <sup>1</sup>	R <sup>2</sup>	Log <i>P</i>	MLOGP	Δ(Log <i>P</i> –MLOGP)	WLOGP	Δ(Log <i>P</i> –WLOGP)
28	Me	Me	3.65	4.26	−0.61	3.47	0.18
29	Me	Ph	4.65	5.31	−0.66	4.17	0.48
30	Et	Et	4.99	5.07	−0.08	4.64	0.35
31	Et	Ph	5.41	5.78	−0.37	4.95	0.46
32	<i>i</i> -Pr	<i>i</i> -Pr	6.06	5.81	0.25	5.81	0.25
33	<i>i</i> -Pr	Ph	6.15	6.24	−0.09	5.73	0.42
34	<i>c</i> -Pr	<i>c</i> -Pr	5.32	5.41	−0.09	4.88	0.44
35	<i>n</i> -Bu	<i>n</i> -Bu	7.50 <sup>a</sup>	6.50	1.00	6.98	0.52
36	<i>c</i> -Pen	<i>c</i> -Pen	7.95 <sup>a</sup>	6.75	1.20	7.41	0.54
37	<i>c</i> -Hex	<i>c</i> -Hex	8.97 <sup>a</sup>	7.37	1.60	8.58	0.39
38	<i>c</i> -Hex	H	7.34 <sup>a</sup>	6.10	1.24	6.45	0.89
39	NMe <sub>2</sub>	NMe <sub>2</sub>	5.64	3.00	2.64	3.01	2.63

<sup>a</sup> These Log*P* values are tentative because the hydrophobicity was beyond the range of the reference compounds (1.9 < Log*P* < 6.5).

Our previous results for *B*-hydroxyphenyl phosphine–borane derivatives indicated that some of these compounds showed Log*P* values with non-negligible differences from the calculated values. Therefore, we calculated the hydrophobicity parameters using SwissADME [48,49]. MLOGP is one of the most representative calculation methods of Log*P* defined by Moriguchi et al. [50,51], which is referred to as Lipinski’s Rule of Five [52,53]. Figure 4A shows the correlation between the measured Log*P* and MLOGP values, with the exception of amide compounds 27 and 39, which is expressed by the following equation:  $\text{Log}P = 1.735\text{MLOGP} - 4.093$  ( $R^2 = 0.911$ ). The correlation coefficient was above 0.9 but not sufficiently large, and moreover, the slope and intercept were significantly large. The difference between the calculated and measured values of each compound ranged from −0.77 (17) to +1.60 (37). MLOGP is a calculation method based on the topology of chemical structures using 13 molecular descriptors that are correlated with Log*P* values. Thereafter, we used the WLOGP calculation method, defined by Wildman and Crippen based on the classification of constituent atoms using 68 atomic descriptors [54]. Figure 4B shows the correlation between the measured Log*P* and WLOGP values, which was expressed by the following equation:  $\text{Log}P = 1.016\text{WLOGP} + 0.271$  ( $R^2 = 0.980$ ). The correlation coefficient was close to 1.0, and the slope and intercept were smaller than those of MLOGP. These results suggest that WLOGP was more suitable for predicting the hydrophobicity of phosphine–borane derivatives.



**Figure 4.** Correlation (A) between experimentally measured Log*P* and calculated MLOGP values and (B) between experimentally measured Log*P* and calculated WLOGP values with the exception of amide derivatives 27 and 39.

#### 2.4. PR Antagonistic Activity

The PR agonistic and antagonistic activities of the synthesized phosphine–borane derivatives were evaluated using an alkaline phosphatase assay with the T47D human breast cancer cell line [55]. None of the test compounds induced alkaline phosphatase activity alone, indicating that they do not act as PR agonists. The basal alkaline phosphatase activity was also not affected by the tested compounds alone. The results also indicated that these compounds exhibited no significant cytotoxicity (Figure S1). The PR antagonistic activities of the compounds were assessed in the presence of 1 nM of P4 (5). We also calculated the molecular volume of each compound to investigate the structure–activity relationship (SAR). Table 2 summarizes the PR antagonistic activity and calculated volumes of the synthesized compounds. All tested compounds exhibited PR antagonistic activity. Among the 3-CF<sub>3</sub> derivatives 16–27, the trimethylphosphine derivative 16, tri-*n*-butylphosphine derivative 23, and tricyclohexylphosphine derivative 25 exhibited only weak potency, and the triethylphosphine derivative 18, diisopropyl(phenyl)phosphine derivative 21, and tricyclopentylphosphine derivative 24 exhibited moderate PR antagonistic activity. The dimethyl(phenyl)phosphine derivative 17, diethyl(phenyl)phosphine derivative 19, triisopropylphosphine derivative 20, and tricyclopropylphosphine derivative 22, as well as the amide derivative 27, exhibited potent activities. These results indicate that the trimethylphosphine moiety cannot sufficiently fill the hydrophobic cavity of the ligand-binding pocket of PR and that the bulky phosphine moiety is too large to enter the ligand-binding pocket. The findings also indicated that phosphines bearing 8–10 carbon atoms are suitable for the hydrophobic substructure of the designed PR antagonists, with the tricyclopropylphosphine substructure as the most suitable hydrophobic motif. The SAR of the 4-CF<sub>3</sub> derivatives 28–39 were similar to those of 3-CF<sub>3</sub> derivatives, and among the synthesized compounds, *B*-(4-trifluoromethyl)phenyl tricyclopropylphosphine–borane (34) was the most potent with an IC<sub>50</sub> value of 0.54 μM. Interestingly, tricyclopropylphosphine derivative 34 was approximately three times more potent than triisopropylphosphine derivative 32 (IC<sub>50</sub> = 1.51 μM). The differences in the molecular volumes of these compounds resulted in large differences in potency. We investigated the binding affinity of the compounds toward the PR ligand-binding domain (LBD) using a fluorescence polarization assay system. Compound 34 exhibited significant affinity toward PR LBD, whereas the less potent compound 28 did not show the affinity, indicating that the potent antagonistic activity of 34 in the alkaline phosphatase assay was mediated by the binding to PR (Figure 5). We also investigated the activity of compounds 28 and 34 toward the androgen receptor (AR) by means of cell-proliferation promoting/inhibitory activity toward androgen-dependent SC-3 cells [56]. These compounds did not affect cell growth both in the presence or absence of dihydrotestosterone, indicating that these compounds did not have AR agonistic or antagonistic activity (Table S1).

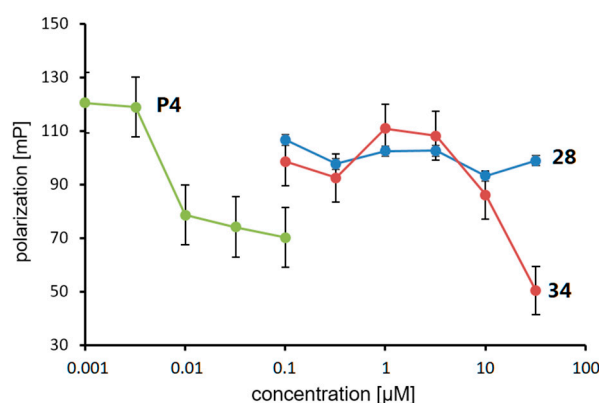
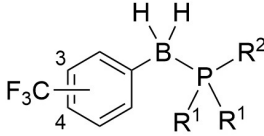


Figure 5. Competitive binding assay using a fluorescence polarization system.

**Table 2.** PR antagonistic activity assessed using a T47D alkaline phosphatase assay and the calculated molecular volumes of synthesized phosphine–borane derivatives 16–39.


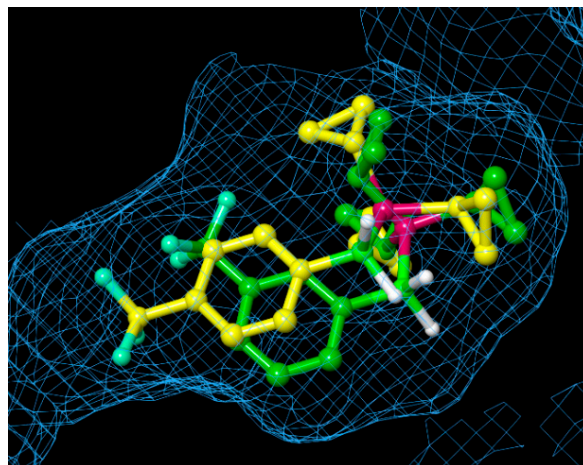
Cmpd	R <sup>1</sup>	R <sup>2</sup>	LogP	Volume (Å <sup>3</sup> ) <sup>a</sup>	IC <sub>50</sub> (μM) <sup>b</sup>
16	Me	Me	3.65	238	>10
17	Me	Ph	4.54	304	1.16 ± 0.60
18	Et	Et	4.88	294	3.67 ± 3.34
19	Et	Ph	5.24	341	1.12 ± 0.22
20	<i>i</i> -Pr	<i>i</i> -Pr	5.89	348	1.35 ± 0.47
21	<i>i</i> -Pr	Ph	5.93	389	3.35 ± 1.49
22	<i>c</i> -Pr	<i>c</i> -Pr	5.21	328	0.65 ± 0.17
23	<i>n</i> -Bu	<i>n</i> -Bu	7.34	404	>10
24	<i>c</i> -Pen	<i>c</i> -Pen	7.84	424	6.64 ± 0.87
25	<i>c</i> -Hex	<i>c</i> -Hex	8.69	474	>10
26	<i>c</i> -Hex	H	7.28	376	N.D. <sup>c</sup>
27	NMe <sub>2</sub>	NMe <sub>2</sub>	5.39	332	1.20 ± 0.63
28	Me	Me	3.65	238	>10
29	Me	Ph	4.65	304	1.61 ± 0.87
30	Et	Et	4.99	294	1.76 ± 1.44
31	Et	Ph	5.41	341	1.78 ± 0.97
32	<i>i</i> -Pr	<i>i</i> -Pr	6.06	347	1.51 ± 0.53
33	<i>i</i> -Pr	Ph	6.15	377	2.01 ± 0.58
34	<i>c</i> -Pr	<i>c</i> -Pr	5.32	328	0.54 ± 0.09
35	<i>n</i> -Bu	<i>n</i> -Bu	7.50	404	>10
36	<i>c</i> -Pen	<i>c</i> -Pen	7.95	424	2.63 ± 0.72
37	<i>c</i> -Hex	<i>c</i> -Hex	8.97	474	>10
38	<i>c</i> -Hex	H	7.34	376	N.D. <sup>c</sup>
39	NMe <sub>2</sub>	NMe <sub>2</sub>	5.64	332	1.40 ± 0.88

<sup>a</sup> These values were calculated for structures optimized at the B3LYP/6-311 + G\*\* level using the Spartan<sup>18</sup> program (Wavefunction, Inc.). <sup>b</sup> The IC<sub>50</sub> values are shown as the mean ± SD from three independent experiments. The P4 concentration was 1.0 nM. <sup>c</sup> Not determined.

### 2.5. Docking Simulations

To estimate the binding mode of the developed phosphine–borane-based PR antagonists, we conducted docking simulations of tricyclopropylphosphine derivatives **22** and **34** with the X-ray crystal structure of the nonsteroidal ligand-bound form of the hPR LBD (PDB ID: 3G8O) using AutoDock 4.2 [57,58]. Figure 6 shows the docking models of phosphine–boranes **22** and **34** in hPR LBD. In the docked structure of *B*-(4-trifluoromethyl)phenyl tricyclopropylphosphine–borane (**34**), the tricyclopropylphosphine moiety occupied the hydrophobic cavity of the ligand-binding pocket, and the 4-(trifluoromethyl)phenyl group was located in the hydrophobic cavity on the contralateral side of the phosphine moiety. In the docked structure of the 3-trifluoromethyl isomer **22**, the tricyclopropylphosphine moiety occupied the hydrophobic cavity in the same manner as that in **34**, and the 3-(trifluoromethyl)phenyl group was located near the center of the pocket. These

results indicated that the tricyclopropylphosphine moiety played an important role in ligand–receptor interactions and that the optimization of the phenyl moiety could lead to the development of novel PR antagonists with improved potency. Overall, a wide variety of phosphine structures, which are difficult to construct using carbon-based functionalities, could enable fine tuning of the hydrophobic interactions, and phosphine–boranes could be a versatile option for the structural optimization of diverse drug candidates.



**Figure 6.** Superimposition of the docked structures of *B*-(3-trifluoromethyl)phenyl tricyclopropylphosphine–borane (**22**: carbon in green) and *B*-(4-trifluoromethyl)phenyl tricyclopropylphosphine–borane (**34**: carbon in yellow), with hPR LBD, calculated using the docking program AutoDock. The protein surface is displayed as a blue mesh.

### 3. Materials and Methods

#### 3.1. Chemistry

All the reagents were purchased from Sigma-Aldrich Inc., St. Louis, MO, USA, Tokyo Chemical Industry Co., Ltd., Tokyo, Japan, Fujifilm Wako Pure Chemical Corporation, Osaka, Japan, or Kanto Chemical Co., Inc., Tokyo, Japan, and used without further purification. Thin-layer chromatography (TLC) was performed using a silica gel coated with the fluorescent indicator F254 (Merck, Boston, MA, USA, #1.05715.0001). Silica gel column chromatography was performed using a neutral silica gel (60 Å, 40–50 µm) purchased from Kanto Chemical Co., Inc. NMR spectra were recorded using Bruker Avance 400 ( $^1\text{H}$ : 400 MHz,  $^{13}\text{C}$ : 100 MHz,  $^{11}\text{B}$ : 128 MHz,  $^{19}\text{F}$ : 376 MHz, and  $^{31}\text{P}$ : 161 MHz) and Bruker Avance 500 ( $^1\text{H}$ : 500 MHz and  $^{13}\text{C}$ : 125 MHz) spectrometers. High-resolution mass (HRMS) spectra were recorded on a Bruker Daltonics micrOTOF-2 focus using electron spray ionization time-of-flight (ESI-TOF).

#### 3.2. General Procedure for the Synthesis of Phosphine–Borane Derivatives 16–39

A dry round-bottomed flask, equipped with a magnetic stirring bar, sealed with a septum, and protected with an Ar balloon, was charged with 4- or 3-(trifluoromethyl)phenyl boronic acid (190 mg, 1.0 mmol or 570 mg, 3.0 mmol) in 1.0 mL of THF. A solution of 1.0 M diisobutyl aluminium hydride (DIBAL) in toluene (3.0 or 5.0 mmol) was added to the mixture, and the corresponding phosphine was added at 0 °C. The mixture was stirred at room temperature and monitored using TLC. Once completed, the reaction was quenched by the addition of a saturated aqueous potassium sodium tartrate solution and extracted with AcOEt. The organic layer was washed with brine and dried over  $\text{Na}_2\text{SO}_4$ . The solvent was evaporated, and the residue was purified using silica gel column chromatography (eluent = hexane/AcOEt) to generate the desired phosphine–borane derivatives. For compounds **20–22** and **32–34**, the corresponding phosphines were prepared immediately before addition, without purification. The details of the characterization and spectra of the compounds are presented in the Supporting Information.

### 3.2.1. *B*-3-(Trifluoromethyl)phenyl Trimethylphosphine–Borane (16)

Colorless oil, Yield 67%, 154 mg;  $^1\text{H}$  NMR (400 MHz, DMSO- $d_6$ ):  $\delta$  7.49–7.46 (m, 2H), 7.37–7.31 (m, 2H), 2.23–1.41 (br, 2H), 1.23 (d,  $J = 11.0$  Hz, 9H);  $^{11}\text{B}$  NMR (128 MHz, DMSO- $d_6$ ):  $\delta$  –23.7 (d,  $J_{\text{BP}} = 59.3$  Hz);  $^{13}\text{C}$  NMR (125 MHz, CDCl<sub>3</sub>):  $\delta$  138.9 (d,  $J_{\text{CP}} = 6.8$  Hz), 131.74–131.66 (m), 129.1 (qd,  $J_{\text{CF}} = 30.8$  Hz,  $J_{\text{CP}} = 3.3$  Hz), 127.2 (d,  $J_{\text{CP}} = 3.4$  Hz), 125.0 (q,  $J_{\text{CF}} = 272.2$  Hz), 121.5–121.4 (m), 10.2 (d,  $J_{\text{CP}} = 37.5$  Hz);  $^{19}\text{F}$  NMR (376 MHz, DMSO- $d_6$ ):  $\delta$  –61.1 (s);  $^{31}\text{P}$  NMR (161 MHz, DMSO- $d_6$ ):  $\delta$  –6.1 (s); HRMS (ESI)  $m/z$  calcd. for C<sub>10</sub>H<sub>15</sub>BF<sub>3</sub>NaP [M + Na]<sup>+</sup> 257.0849, found 257.0852.

### 3.2.2. *B*-(3-Trifluoromethyl)phenyl Dimethyl(phenyl)phosphine–Borane (17)

White solid; Yield 68%, 177 mg; MP 75.0–75.8 °C;  $^1\text{H}$  NMR (400 MHz, DMSO- $d_6$ )  $\delta$  7.65 (t,  $J = 8.7$  Hz, 2H), 7.57–7.43 (m, 4H), 7.36–7.26 (m, 3H), 2.35–1.72 (br, 2H), 1.53 (d,  $J = 10.7$  Hz, 6H);  $^{11}\text{B}$  NMR (128 MHz, DMSO- $d_6$ )  $\delta$  –23.8 (s);  $^{13}\text{C}$  NMR (125 MHz, CDCl<sub>3</sub>)  $\delta$  139.2 (d,  $J_{\text{CP}} = 7.0$  Hz), 132.1–132.0 (m), 131.3 (d,  $J_{\text{CP}} = 2.4$  Hz), 130.8 (d,  $J_{\text{CP}} = 8.4$  Hz), 129.3 (d,  $J_{\text{CP}} = 53.5$  Hz), 129.1 (qd,  $J_{\text{CF}} = 31.0$  Hz,  $J_{\text{CP}} = 3.3$  Hz), 128.9 (d,  $J_{\text{CP}} = 10$  Hz), 127.2 (d,  $J_{\text{CP}} = 3.4$  Hz), 124.9 (q,  $J_{\text{CF}} = 272.1$  Hz), 121.6–121.5 (m), 10.0 (d,  $J_{\text{CP}} = 38.2$  Hz);  $^{19}\text{F}$  NMR (376 MHz, DMSO- $d_6$ )  $\delta$  –61.1 (s);  $^{31}\text{P}$  NMR (161 MHz, DMSO- $d_6$ )  $\delta$  –1.2 (s); HRMS (ESI)  $m/z$  calcd. for C<sub>15</sub>H<sub>17</sub>BF<sub>3</sub>NaP [M + Na]<sup>+</sup> 319.1005, found 319.0998.

### 3.2.3. *B*-3-(Trifluoromethyl)phenyl Triethylphosphine–Borane (18)

Colorless oil; Yield 26%, 71 mg;  $^1\text{H}$  NMR (400 MHz, DMSO- $d_6$ )  $\delta$  7.50–7.48 (m, 2H), 7.35–7.29 (m, 2H), 1.63–1.54 (m, 6H), 1.04–0.96 (m, 9H);  $^{11}\text{B}$  NMR (128 MHz, DMSO- $d_6$ )  $\delta$  –27.4 (d,  $J_{\text{BP}} = 50.1$  Hz);  $^{13}\text{C}$  NMR (125 MHz, CDCl<sub>3</sub>)  $\delta$  139.1 (d,  $J_{\text{CP}} = 6.4$  Hz), 132.0–131.9 (m), 129.0 (qd,  $J_{\text{CF}} = 30.9$  Hz,  $J_{\text{CP}} = 3.0$  Hz), 127.1 (d,  $J_{\text{CP}} = 2.9$  Hz), 125.0 (q,  $J_{\text{CF}} = 272.3$  Hz), 121.3–121.2 (m), 12.8 (d,  $J_{\text{CP}} = 34.1$  Hz), 6.4 (d,  $J_{\text{CP}} = 3.9$  Hz);  $^{19}\text{F}$  NMR (376 MHz, DMSO- $d_6$ )  $\delta$  –61.1 (s);  $^{31}\text{P}$  NMR (161 MHz, DMSO- $d_6$ )  $\delta$  12.5 (s); HRMS (ESI)  $m/z$  calcd. for C<sub>13</sub>H<sub>21</sub>BF<sub>3</sub>NaP [M + Na]<sup>+</sup> 299.1318, found 299.1325.

### 3.2.4. *B*-3-(Trifluoromethyl)phenyl Diethyl(phenyl)phosphine–Borane (19)

White solid; Yield 68%, 215 mg; MP 40.0–40.5 °C;  $^1\text{H}$  NMR (400 MHz, CD<sub>2</sub>Cl<sub>2</sub>)  $\delta$  7.62–7.58 (m, 2H), 7.56–7.46 (m, 5H), 7.30 (d,  $J = 7.5$  Hz, 1H), 7.23 (t,  $J = 7.5$  Hz, 1H), 1.89–1.76 (m, 4H), 1.09–1.01 (m, 6H);  $^{11}\text{B}$  NMR (128 MHz, DMSO- $d_6$ )  $\delta$  –27.1 (s);  $^{13}\text{C}$  NMR (100 MHz, DMSO- $d_6$ ):  $\delta$  139.8 (d,  $J_{\text{CP}} = 6.4$  Hz), 132.5 (d,  $J_{\text{CP}} = 7.6$  Hz), 131.9–131.7 (m), 131.7 (d,  $J_{\text{CP}} = 2.2$  Hz), 129.3 (d,  $J_{\text{CP}} = 9.3$  Hz), 128.2 (qd,  $J_{\text{CF}} = 30.3$  Hz,  $J_{\text{CP}} = 3.1$  Hz), 127.9 (d,  $J_{\text{CP}} = 3.0$  Hz), 126.4 (d,  $J_{\text{CP}} = 51.1$  Hz), 125.3 (q,  $J_{\text{CF}} = 272.2$  Hz), 121.5–121.4 (m), 14.5 (d,  $J_{\text{CP}} = 36.0$  Hz), 6.9 (d,  $J_{\text{CP}} = 3.0$  Hz);  $^{19}\text{F}$  NMR (376 MHz, DMSO- $d_6$ )  $\delta$  –61.2 (s);  $^{31}\text{P}$  NMR (161 MHz, DMSO- $d_6$ )  $\delta$  13.1 (s); ESMS (ESI)  $m/z$  calcd. for C<sub>17</sub>H<sub>21</sub>BF<sub>3</sub>NaP [M + Na]<sup>+</sup> 347.1318, found 347.1310.

### 3.2.5. *B*-3-(Trifluoromethyl)phenyl Triisopropylphosphine–Borane (20)

Colorless oil; Yield 54%, 514 mg (2 steps);  $^1\text{H}$  NMR (400 MHz, DMSO- $d_6$ )  $\delta$  7.57–7.55 (m, 2H), 7.34–7.28 (m, 2H), 2.28–1.50 (br, 2H), 2.26–2.16 (m, 3H), 1.17–1.12 (m, 18H);  $^{11}\text{B}$  NMR (128 MHz, DMSO- $d_6$ )  $\delta$  –28.8 (s);  $^{13}\text{C}$  NMR (125 MHz, DMSO- $d_6$ )  $\delta$  140.2 (d,  $J_{\text{CP}} = 5.5$  Hz), 132.3–132.2 (m), 128.0 (qd,  $J_{\text{CF}} = 30.2$  Hz,  $J_{\text{CP}} = 3.4$  Hz), 127.9 (d,  $J_{\text{CP}} = 3.0$  Hz), 125.4 (q,  $J_{\text{CF}} = 272.2$  Hz), 121.31–121.25 (m), 20.6 (d,  $J_{\text{CP}} = 29.5$  Hz), 18.1 (d,  $J_{\text{CP}} = 1.5$  Hz);  $^{19}\text{F}$  NMR (376 MHz, DMSO- $d_6$ )  $\delta$  –61.2 (s);  $^{31}\text{P}$  NMR (161 MHz, DMSO- $d_6$ )  $\delta$  24.6 (s); HRMS (ESI)  $m/z$  calcd. for C<sub>16</sub>H<sub>27</sub>BF<sub>3</sub>NaP [M + Na]<sup>+</sup> 341.1788, found 341.1800.

### 3.2.6. *B*-3-(Trifluoromethyl)phenyl Diisopropyl(phenyl)phosphine–Borane (21)

White solid; Yield 25%, 263 mg (2 step); MP 118.7–119.1 °C;  $^1\text{H}$  NMR (400 MHz, CD<sub>2</sub>Cl<sub>2</sub>)  $\delta$  7.80–7.76 (m, 2H), 7.69 (s, 1H), 7.62 (d,  $J = 6.9$  Hz, 1H), 7.59–7.50 (m, 3H), 7.29 (d,  $J = 7.3$  Hz, 1H), 7.22 (t,  $J = 7.5$  Hz, 1H), 2.72–1.90 (br, 2H), 2.49–2.39 (m, 2H), 1.08–0.95 (m, 12H);  $^{11}\text{B}$  NMR (128 MHz, DMSO- $d_6$ )  $\delta$  –28.5 (s);  $^{13}\text{C}$  NMR (100 MHz, DMSO- $d_6$ )  $\delta$  140.2 (d,  $J_{\text{CP}} = 6.8$  Hz), 134.1 (d,  $J_{\text{CP}} = 6.7$  Hz), 132.3–132.2 (m), 132.0 (d,  $J_{\text{CP}} = 2.2$  Hz),

129.2 (d,  $J_{CP} = 8.9$  Hz), 128.2 (qd,  $J_{CF} = 27.6$  Hz,  $J_{CP} = 2.5$  Hz), 127.9 (d,  $J_{CP} = 2.2$  Hz), 125.4 (q,  $J_{CF} = 272.2$  Hz), 123.5 (d,  $J_{CP} = 46.9$  Hz), 121.53–121.46 (m), 20.7 (d,  $J_{CP} = 32.7$  Hz), 16.8–16.7 (m);  $^{19}\text{F}$  NMR (376 MHz, DMSO- $d_6$ )  $\delta$  -61.2 (s);  $^{31}\text{P}$  NMR (161 MHz, DMSO- $d_6$ )  $\delta$  22.1 (s); HRMS (ESI)  $m/z$  calcd. for  $\text{C}_{19}\text{H}_{25}\text{BF}_3\text{NaP}$   $[\text{M} + \text{Na}]^+$  375.1631, found 375.1653.

### 3.2.7. B-3-(Trifluoromethyl)phenyl Tricyclopropylphosphine-Borane (22)

Colorless oil; Yield 26%, 80 mg (2 steps);  $^1\text{H}$  NMR (400 MHz, DMSO- $d_6$ )  $\delta$  7.54–7.52 (m, 2H), 7.34–7.26 (m, 2H), 2.00–1.05 (br, 2H), 0.80–0.62 (m, 15H);  $^{11}\text{B}$  NMR (128 MHz, DMSO- $d_6$ )  $\delta$  -29.1 (s);  $^{13}\text{C}$  NMR (125 MHz,  $\text{CDCl}_3$ )  $\delta$  139.5 (d,  $J_{CP} = 6.9$  Hz), 132.5–132.4 (m), 128.7 (q,  $J_{CF} = 31.4$  Hz), 126.9 (d,  $J_{CP} = 2.5$  Hz), 125.0 (q,  $J_{CF} = 272.3$  Hz), 121.1–121.0 (m), 2.1 (d,  $J_{CP} = 3.0$  Hz), 1.6 (d,  $J_{CP} = 58.3$  Hz);  $^{19}\text{F}$  NMR (376 MHz, DMSO- $d_6$ )  $\delta$  -61.1 (s);  $^{31}\text{P}$  NMR (161 MHz, DMSO- $d_6$ )  $\delta$  17.3 (s); HRMS (ESI)  $m/z$  calcd. for  $\text{C}_{16}\text{H}_{21}\text{BF}_3\text{NaP}$   $[\text{M} + \text{Na}]^+$  335.1318, found 335.1323.

### 3.2.8. B-3-(Trifluoromethyl)phenyl Tri-*n*-Butylphosphine-Borane (23)

Colorless oil; Yield 66%, 238 mg;  $^1\text{H}$  NMR (400 MHz, DMSO- $d_6$ )  $\delta$  7.47 (s, 2H), 7.36–7.30 (m, 2H), 1.57–1.51 (m, 6H), 1.38–1.29 (m, 12H), 0.85 (t,  $J = 7.0$  Hz, 9H);  $^{11}\text{B}$  NMR (128 MHz, DMSO- $d_6$ )  $\delta$  -26.8 (s);  $^{13}\text{C}$  NMR (125 MHz,  $\text{CDCl}_3$ )  $\delta$  139.0 (d,  $J_{CP} = 6.4$  Hz), 132.0–131.9 (m), 128.9 (qd,  $J_{CF} = 30.8$  Hz,  $J_{CP} = 3.4$  Hz), 127.1 (d,  $J_{CP} = 3.4$  Hz), 125.0 (q,  $J_{CF} = 272.2$  Hz), 121.2–121.1 (m), 24.4 (d,  $J_{CP} = 2.8$  Hz), 24.3 (d,  $J_{CP} = 12.5$  Hz), 20.2 (d,  $J_{CP} = 33.0$  Hz), 13.4 (s);  $^{19}\text{F}$  NMR (376 MHz, DMSO- $d_6$ )  $\delta$  -61.2 (s);  $^{31}\text{P}$  NMR (161 MHz, DMSO- $d_6$ )  $\delta$  7.03 (s); ESMS (ESI)  $m/z$  calcd. for  $\text{C}_{19}\text{H}_{33}\text{BF}_3\text{NaP}$   $[\text{M} + \text{Na}]^+$  383.2257, found 383.2276.

### 3.2.9. B-3-(Trifluoromethyl)phenyl Tricyclopentylphosphine-Borane (24)

Colorless oil; Yield 60%, 239 mg;  $^1\text{H}$  NMR (400 MHz, DMSO- $d_6$ )  $\delta$  7.56–7.53 (m, 2H), 7.32–7.26 (m, 2H), 2.23–1.69 (br, 2H), 2.19–2.10 (m, 3H), 1.81–1.79 (m, 6H), 1.58–1.50 (m, 18H);  $^{11}\text{B}$  NMR (128 MHz, DMSO- $d_6$ )  $\delta$  -28.4 (s);  $^{13}\text{C}$  NMR (125 MHz,  $\text{CDCl}_3$ )  $\delta$  139.6 (d,  $J_{CP} = 6.0$  Hz), 132.8–132.7 (m), 128.7 (qd,  $J_{CF} = 30.7$  Hz,  $J_{CP} = 2.9$  Hz), 126.8 (d,  $J_{CP} = 2.8$  Hz), 125.0 (q,  $J_{CF} = 272.3$  Hz), 121.0–120.9 (m), 32.4 (d,  $J_{CP} = 31.9$  Hz), 28.3 (s), 26.0 (d,  $J_{CP} = 8.8$  Hz);  $^{19}\text{F}$  NMR (376 MHz, DMSO- $d_6$ )  $\delta$  -61.2 (s);  $^{31}\text{P}$  NMR (161 MHz, DMSO- $d_6$ )  $\delta$  19.1 (s); HRMS (ESI)  $m/z$  calcd. for  $\text{C}_{22}\text{H}_{33}\text{BF}_3\text{NaP}$   $[\text{M} + \text{Na}]^+$  419.2257, found 419.2265.

### 3.2.10. B-3-(Trifluoromethyl)phenyl Tricyclohexylphosphine-Borane (25)

White solid; Yield:45%, 213 mg; MP 100.0–100.5 °C;  $^1\text{H}$  NMR (400 MHz, DMSO- $d_6$ )  $\delta$  7.53 (s, 2H), 7.35–7.30 (m, 2H), 2.08–1.10 (br, 2H), 1.94–1.65 (m, 18H), 1.32–1.14 (m, 15H);  $^{11}\text{B}$  NMR (128 MHz, DMSO- $d_6$ )  $\delta$  -28.8 (s);  $^{13}\text{C}$  NMR (125 MHz, DMSO- $d_6$ )  $\delta$  140.2 (d,  $J_{CP} = 5.2$  Hz), 132.4–132.3 (m), 128.0 (qd,  $J_{CF} = 30.1$  Hz,  $J_{CP} = 2.6$  Hz), 128.0 (d,  $J_{CP} = 2.3$  Hz), 125.5 (q,  $J_{CF} = 272.6$  Hz), 121.33–121.27 (m), 30.3 (d,  $J_{CP} = 28.7$  Hz), 27.8 (d,  $J_{CP} = 1.4$  Hz), 27.2 (d,  $J_{CP} = 10.0$  Hz), 26.1 (s);  $^{19}\text{F}$  NMR (376 MHz, DMSO- $d_6$ )  $\delta$  -61.2 (s);  $^{31}\text{P}$  NMR (161 MHz, DMSO- $d_6$ )  $\delta$  15.7 (s); HRMS (ESI)  $m/z$  calcd. for  $\text{C}_{25}\text{H}_{39}\text{BF}_3\text{NaP}$   $[\text{M} + \text{Na}]^+$  461.2727, found 461.2739.

### 3.2.11. B-3-(Trifluoromethyl)phenyl Dicyclohexylphosphine-Borane (26)

Colorless oil; Yield 31%, 109 mg;  $^1\text{H}$  NMR (400 MHz, acetone- $d_6$ )  $\delta$  7.65–7.60 (m, 2H), 7.35–7.28 (m, 2H), 4.26 (d,  $J = 357.0$  Hz, 1H), 2.82–1.66 (br, 2H), 2.12–2.01 (m, 2H), 1.85–1.66 (m, 10H), 1.47–1.15 (m, 10H);  $^{11}\text{B}$  NMR (128 MHz, DMSO- $d_6$ )  $\delta$  -29.18 (s);  $^{13}\text{C}$  NMR (100 MHz, acetone- $d_6$ )  $\delta$  140.4 (d,  $J_{CP} = 7.0$  Hz), 132.8–132.7 (m), 129.5 (qd,  $J_{CF} = 30.3$  Hz,  $J_{CP} = 2.9$  Hz), 128.3 (d,  $J_{CP} = 2.6$  Hz), 126.2 (q,  $J_{CF} = 271.5$  Hz), 121.9–121.8 (m), 30.7 (s), 29.8 (d,  $J_{CP} = 31.1$  Hz), 29.1 (s), 27.4 (d,  $J_{CP} = 10.3$  Hz), 27.2 (d,  $J_{CP} = 11.5$  Hz), 26.5 (s);  $^{19}\text{F}$  NMR (376 MHz, DMSO- $d_6$ )  $\delta$  -61.12 (s);  $^{31}\text{P}$  NMR (161 MHz, DMSO- $d_6$ )  $\delta$  10.0 (d,  $J = 353.3$  Hz); HRMS (ESI)  $m/z$  calcd. for  $\text{C}_{19}\text{H}_{29}\text{BF}_3\text{NaP}$   $[\text{M} + \text{Na}]^+$  379.1944, found 379.1929.

### 3.2.12. B-3-(Trifluoromethyl)phenyl Tris(dimethylamino)phosphine–Borane (27)

Colorless oil; Yield:23%, 75 mg;  $^1\text{H}$  NMR (400 MHz, DMSO- $d_6$ )  $\delta$  7.57–7.53 (m, 2H), 7.33–7.527 (m, 2H), 2.52 (d,  $J = 9.1$  Hz, 18H), 2.30–1.56 (br, 2H);  $^{11}\text{B}$  NMR (128 MHz, DMSO- $d_6$ )  $\delta$  –27.1 (d,  $J = 104.8$  Hz);  $^{13}\text{C}$  NMR (125 MHz, DMSO- $d_6$ ):  $\delta$  140.3 (d,  $J_{\text{CP}} = 8.1$  Hz), 132.3–132.2 (m), 127.8 (qd,  $J_{\text{CF}} = 30.3$  Hz,  $J_{\text{CP}} = 2.9$  Hz), 127.7 (s), 125.5 (q,  $J_{\text{CF}} = 272.2$  Hz), 121.18–121.12 (m), 37.3 (d,  $J_{\text{CP}} = 3.4$  Hz);  $^{19}\text{F}$  NMR (376 MHz, DMSO- $d_6$ )  $\delta$  –61.1 (s);  $^{31}\text{P}$  NMR (161 MHz, DMSO- $d_6$ )  $\delta$  92.3 (s); HRMS (ESI)  $m/z$  calcd. for  $\text{C}_{13}\text{H}_{24}\text{BF}_3\text{N}_3\text{NaP}$   $[\text{M} + \text{Na}]^+$  344.1645, found 344.1640.

### 3.2.13. B-4-(Trifluoromethyl)phenyl Trimethylphosphine–Borane (28)

Colorless oil; Yield: 24%, 55 mg;  $^1\text{H}$  NMR (400 MHz, DMSO- $d_6$ )  $\delta$  7.41 (s, 4H), 2.29–1.42 (br, 2H), 1.23 (d,  $J = 10.9$  Hz, 9H);  $^{11}\text{B}$  NMR (128 MHz, DMSO- $d_6$ ):  $\delta$  –23.8 (d,  $J_{\text{BP}} = 63.1$  Hz);  $^{13}\text{C}$  NMR (125 MHz,  $\text{CDCl}_3$ )  $\delta$  135.6 (d,  $J_{\text{CP}} = 7.0$  Hz), 126.8 (qd,  $J_{\text{CF}} = 31.5$  Hz,  $J_{\text{CP}} = 4.7$  Hz), 125.0 (qd,  $J_{\text{CF}} = 271.3$  Hz,  $J_{\text{CP}} = 1.7$  Hz), 123.7 (s), 10.3 (d,  $J_{\text{CP}} = 37.5$  Hz);  $^{19}\text{F}$  NMR (376 MHz, DMSO- $d_6$ )  $\delta$  –55.9 (s);  $^{31}\text{P}$  NMR (161 MHz, DMSO- $d_6$ )  $\delta$  –6.2 (s); HRMS (ESI)  $m/z$  calcd. for  $\text{C}_{10}\text{H}_{15}\text{BF}_3\text{NaP}$   $[\text{M} + \text{Na}]^+$  257.0849, found 257.0842.

### 3.2.14. B-4-(Trifluoromethyl)phenyl Dimethyl(phenyl)phosphine–Borane (29)

White solid; Yield:28%, 73 mg; MP 78.0–78.3 °C;  $^1\text{H}$  NMR (400 MHz, DMSO- $d_6$ )  $\delta$  7.69–7.66 (m, 2H), 7.58–7.49 (m, 3H), 7.38 (s, 4H), 2.30–1.72 (br, 2H), 1.54 (d,  $J = 10.7$  Hz, 6H);  $^{11}\text{B}$  NMR (128 MHz, DMSO- $d_6$ )  $\delta$  –23.8 (s);  $^{13}\text{C}$  NMR (100 MHz, DMSO- $d_6$ )  $\delta$  136.3 (d,  $J_{\text{CP}} = 7.2$  Hz), 131.6 (d,  $J_{\text{CP}} = 2.1$  Hz), 131.4 (d,  $J_{\text{CP}} = 8.8$  Hz), 130.1 (d,  $J_{\text{CP}} = 54.4$  Hz), 129.3 (d,  $J_{\text{CP}} = 9.6$  Hz), 125.7 (qd,  $J_{\text{CF}} = 31.2$  Hz,  $J_{\text{CP}} = 4.3$  Hz), 125.5 (qd,  $J_{\text{CF}} = 270.9$  Hz,  $J_{\text{CP}} = 1.3$  Hz), 123.67–13.60 (m), 9.7 (d,  $J_{\text{CP}} = 38.8$  Hz);  $^{19}\text{F}$  NMR (376 MHz, DMSO- $d_6$ )  $\delta$  –60.8 (d,  $J = 4.1$  Hz);  $^{31}\text{P}$  NMR (161 MHz, DMSO- $d_6$ )  $\delta$  –1.4 (s); HRMS (ESI)  $m/z$  calcd. for  $\text{C}_{15}\text{H}_{17}\text{BF}_3\text{NaP}$   $[\text{M} + \text{Na}]^+$  319.1005, found 319.1013.

### 3.2.15. B-4-(Trifluoromethyl)phenyl Triethylphosphine–Borane (30)

Colorless oil; Yield:49%, 135 mg;  $^1\text{H}$  NMR (400 MHz, DMSO- $d_6$ )  $\delta$  7.41 (s, 4H), 2.24–1.43 (br, 2H), 1.63–1.55 (m, 6H), 1.05–0.97 (m, 9H);  $^{11}\text{B}$  NMR (128 MHz, DMSO- $d_6$ )  $\delta$  –27.6 (d,  $J_{\text{BP}} = 53.0$  Hz);  $^{13}\text{C}$  NMR (125 MHz,  $\text{CDCl}_3$ )  $\delta$  135.8 (d,  $J_{\text{CP}} = 6.6$  Hz), 126.5 (qd,  $J_{\text{CF}} = 31.7$  Hz,  $J_{\text{CP}} = 4.2$  Hz), 125.0 (qd,  $J_{\text{CF}} = 271.6$  Hz), 123.6–123.5 (m), 12.8 (d,  $J_{\text{CP}} = 34.1$  Hz), 6.4 (d,  $J_{\text{CP}} = 3.8$  Hz);  $^{19}\text{F}$  NMR (376 MHz, DMSO- $d_6$ )  $\delta$  –60.7 (d,  $J_{\text{FP}} = 3.0$  Hz);  $^{31}\text{P}$  NMR (161 MHz, DMSO- $d_6$ )  $\delta$  12.8 (s); HRMS (ESI)  $m/z$  calcd. for  $\text{C}_{13}\text{H}_{21}\text{BF}_3\text{NaP}$   $[\text{M} + \text{Na}]^+$  299.1318, found 299.1319.

### 3.2.16. B-4-(Trifluoromethyl)phenyl Diethyl(phenyl)phosphine–Borane (31)

White solid; Yield:38%, 121 mg; MP 62.0–62.3 °C;  $^1\text{H}$  NMR (400 MHz, DMSO- $d_6$ )  $\delta$  7.75–7.70 (m, 2H), 7.61–7.52 (m, 3H), 7.39 (s, 4H), 2.45–1.76 (br, 2H), 2.02–1.77 (m, 4H), 0.98–0.90 (m, 6H);  $^{11}\text{B}$  NMR (128 MHz, DMSO- $d_6$ )  $\delta$  –27.3 (s);  $^{13}\text{C}$  NMR (125 MHz,  $\text{CDCl}_3$ )  $\delta$  135.9 (d,  $J_{\text{CP}} = 7.1$  Hz), 132.1 (d,  $J_{\text{CP}} = 7.5$  Hz), 131.3 (d,  $J_{\text{CP}} = 2.5$  Hz), 128.9 (d,  $J_{\text{CP}} = 9.4$  Hz), 126.8 (qd,  $J_{\text{CF}} = 31.7$  Hz,  $J_{\text{CP}} = 4.2$  Hz), 126.1 (d,  $J_{\text{CP}} = 50.3$  Hz), 125.0 (q,  $J_{\text{CF}} = 271.5$  Hz), 123.61–123.56 (m), 15.1 (d,  $J_{\text{CP}} = 35.6$  Hz), 6.7 (d,  $J_{\text{CP}} = 3.0$  Hz);  $^{19}\text{F}$  NMR (376 MHz, DMSO- $d_6$ )  $\delta$  –60.7 (d,  $J = 3.8$  Hz);  $^{31}\text{P}$  NMR (161 MHz, DMSO- $d_6$ )  $\delta$  13.3 (s); ESMS (ESI)  $m/z$  calcd. for  $\text{C}_{17}\text{H}_{21}\text{BF}_3\text{PNa}$   $[\text{M} + \text{Na}]^+$  347.1318, found 347.1317.

### 3.2.17. B-4-(Trifluoromethyl)phenyl Triisopropylphosphine–Borane (32)

White solid; Yield:13%, 123 mg (2 steps); MP 59.0–59.4 °C;  $^1\text{H}$  NMR (400 MHz, DMSO- $d_6$ )  $\delta$  7.49 (d,  $J = 7.4$  Hz, 2H), 7.39 (d,  $J = 8.0$  Hz, 2H), 2.30–1.52 (br, 2H), 2.28–2.18 (m, 3H), 1.17–1.12 (m, 18H);  $^{11}\text{B}$  NMR (128 MHz, DMSO- $d_6$ )  $\delta$  –28.7 (d,  $J = 37.6$  Hz);  $^{13}\text{C}$  NMR (125 MHz,  $\text{CDCl}_3$ )  $\delta$  136.3 (d,  $J_{\text{CP}} = 6.2$  Hz), 126.5 (q,  $J_{\text{CF}} = 30.0$  Hz), 125.1 (q,  $J_{\text{CF}} = 271.4$  Hz), 123.4 (s), 20.8 (d,  $J_{\text{CP}} = 29.2$  Hz), 18.0 (s);  $^{19}\text{F}$  NMR (376 MHz, DMSO- $d_6$ )  $\delta$  –60.6 (d,  $J = 3.5$  Hz);  $^{31}\text{P}$  NMR (161 MHz, DMSO- $d_6$ )  $\delta$  24.9 (s); HRMS (ESI)  $m/z$  calcd. for  $\text{C}_{16}\text{H}_{27}\text{BF}_3\text{NaP}$   $[\text{M} + \text{Na}]^+$  341.1788, found 341.1791.

**3.2.18. B-4-(Trifluoromethyl)phenyl Diisopropyl(phenyl)phosphine–Borane (33)**

White solid; Yield 18%, 186 mg (2 steps); MP 94.8–95.2 °C;  $^1\text{H}$  NMR (400 MHz, DMSO- $d_6$ )  $\delta$  7.87–7.65 (m, 2H), 7.65–7.57 (m, 3H), 7.52 (d,  $J = 7.1$  Hz, 2H), 7.39 (d,  $J = 8.0$  Hz, 2H), 2.65–2.00 (br, 2H), 2.63–2.53 (m, 2H), 1.01–0.86 (m, 12H);  $^{11}\text{B}$  NMR (128 MHz, DMSO- $d_6$ )  $\delta$  –28.9 (s);  $^{13}\text{C}$  NMR (125 MHz,  $\text{CDCl}_3$ )  $\delta$  136.3 (d,  $J_{\text{CP}} = 7.0$  Hz), 133.6 (d,  $J_{\text{CP}} = 6.5$  Hz), 131.3 (d,  $J_{\text{CP}} = 2.4$  Hz), 128.6 (d,  $J_{\text{CP}} = 8.7$  Hz), 126.7 (qd,  $J_{\text{CF}} = 31.8$  Hz,  $J_{\text{CP}} = 3.8$  Hz), 125.0 (q,  $J_{\text{CF}} = 271.2$  Hz), 123.9 (s), 123.53–123.48 (m), 21.2 (d,  $J_{\text{CP}} = 31.8$  Hz), 16.7–16.5 (m);  $^{19}\text{F}$  NMR (376 MHz, DMSO- $d_6$ )  $\delta$  –60.7 (d,  $J = 2.8$  Hz);  $^{31}\text{P}$  NMR (161 MHz, DMSO- $d_6$ )  $\delta$  22.5 (s); HRMS (ESI)  $m/z$  calcd. for  $\text{C}_{19}\text{H}_{25}\text{BF}_3\text{NaP}$   $[\text{M} + \text{Na}]^+$  375.1631, found 375.1632.

**3.2.19. B-4-(Trifluoromethyl)phenyl Tricyclopropylphosphine–Borane (34)**

White solid; Yield:22%, 68 mg (2 steps); MP 72.6–72.8 °C;  $^1\text{H}$  NMR (400 MHz, DMSO- $d_6$ )  $\delta$  7.46 (d,  $J = 6.9$  Hz, 2H), 7.38 (d,  $J = 8.1$  Hz, 2H), 1.99–1.12 (br, 2H), 0.81–0.66 (m, 15H);  $^{11}\text{B}$  NMR (128 MHz, DMSO- $d_6$ )  $\delta$  –29.4 (s);  $^{13}\text{C}$  NMR (125 MHz, DMSO- $d_6$ )  $\delta$  136.6 (d,  $J_{\text{CP}} = 6.8$  Hz), 125.5 (qd,  $J_{\text{CF}} = 271.4$  Hz), 125.4 (qd,  $J_{\text{CF}} = 31.1$  Hz,  $J_{\text{CP}} = 4.1$  Hz), 123.42–123.39 (m), 2.37 (d,  $J_{\text{CP}} = 3.3$  Hz), 1.65 (d,  $J_{\text{CP}} = 59.3$  Hz);  $^{19}\text{F}$  NMR (376 MHz, DMSO- $d_6$ )  $\delta$  –60.6 (d,  $J = 4.0$  Hz);  $^{31}\text{P}$  NMR (161 MHz, DMSO- $d_6$ )  $\delta$  17.7 (s); HRMS (ESI)  $m/z$  calcd. for  $\text{C}_{16}\text{H}_{21}\text{BF}_3\text{NaP}$   $[\text{M} + \text{Na}]^+$  335.1318, found 335.1321.

**3.2.20. B-4-(Trifluoromethyl)phenyl Tri-*n*-butylphosphine–Borane (35)**

White solid; Yield:15%, 54 mg; MP 33.2–33.8 °C;  $^1\text{H}$  NMR (400 MHz, DMSO- $d_6$ )  $\delta$  7.41 (s, 4H), 1.59–1.52 (m, 6H), 2.10–1.48 (br, 2H), 1.38–1.29 (m, 12H), 0.85 (t,  $J = 7.0$  Hz, 9H);  $^{11}\text{B}$  NMR (128 MHz, DMSO- $d_6$ )  $\delta$  –26.8 (s);  $^{13}\text{C}$  NMR (125 MHz, DMSO- $d_6$ )  $\delta$  136.2 (d,  $J_{\text{CP}} = 6.6$  Hz), 125.54 (q,  $J_{\text{CF}} = 270.9$  Hz), 125.48 (qd,  $J_{\text{CF}} = 31.1$  Hz,  $J_{\text{CP}} = 4.0$  Hz), 123.7–123.6 (m), 24.43 (d,  $J_{\text{CP}} = 2.7$  Hz), 24.37 (d,  $J_{\text{CP}} = 12.5$  Hz), 20.1 (d,  $J_{\text{CP}} = 33.8$  Hz), 13.9 (s);  $^{19}\text{F}$  NMR (376 MHz, DMSO- $d_6$ )  $\delta$  –60.7 (s);  $^{31}\text{P}$  NMR (161 MHz, DMSO- $d_6$ )  $\delta$  7.4 (s); ESMS (ESI) calcd. for  $\text{C}_{19}\text{H}_{33}\text{BF}_3\text{PNa}$   $[\text{M} + \text{Na}]^+$  383.2257, found 383.2270.

**3.2.21. B-4-(Trifluoromethyl)phenyl Tricyclopentylphosphine–Borane (36)**

White solid; Yield:32%, 126 mg; MP 88.0–88.6 °C;  $^1\text{H}$  NMR (400 MHz, DMSO- $d_6$ )  $\delta$  7.48 (d,  $J = 7.0$  Hz, 2H), 7.38 (d,  $J = 7.8$  Hz, 2H), 2.24–1.73 (br, 2H), 2.20–2.12 (m, 3H), 1.82–1.80 (m, 6H), 1.58–1.50 (m, 18H);  $^{11}\text{B}$  NMR (128 MHz, DMSO- $d_6$ )  $\delta$  –28.9 (s);  $^{13}\text{C}$  NMR (125 MHz,  $\text{CDCl}_3$ )  $\delta$  136.4 (d,  $J_{\text{CP}} = 6.0$  Hz), 126.4 (qd,  $J_{\text{CF}} = 31.6$  Hz,  $J_{\text{CP}} = 4.0$  Hz), 125.1 (q,  $J_{\text{CF}} = 271.1$  Hz), 123.31–123.26 (m), 34.3 (d,  $J_{\text{CP}} = 32.0$  Hz), 28.4 (s), 26.1 (d,  $J_{\text{CP}} = 8.4$  Hz);  $^{19}\text{F}$  NMR (376 MHz, DMSO- $d_6$ )  $\delta$  –60.9 (t,  $J = 2.3$  Hz);  $^{31}\text{P}$  NMR (161 MHz, DMSO- $d_6$ )  $\delta$  19.4 (s); HRMS (ESI)  $m/z$  calcd. for  $\text{C}_{22}\text{H}_{33}\text{BF}_3\text{NaP}$   $[\text{M} + \text{Na}]^+$  419.2257, found 419.2247.

**3.2.22. B-4-(Trifluoromethyl)phenyl Tricyclohexylphosphine–Borane (37)**

White solid; Yield:29%, 140 mg; MP 126.7–127.0 °C;  $^1\text{H}$  NMR (400 MHz, DMSO- $d_6$ )  $\delta$  7.47–7.40 (m, 4H), 1.98–1.10 (br, 2H), 1.93–1.65 (m, 18H), 1.32–1.20 (m, 15H);  $^{11}\text{B}$  NMR (128 MHz, DMSO- $d_6$ )  $\delta$  –28.8 (s);  $^{13}\text{C}$  NMR (125 MHz, DMSO- $d_6$ ):  $\delta$  136.8 (d,  $J_{\text{CP}} = 6.3$  Hz), 125.5 (d,  $J_{\text{CF}} = 271.7$  Hz), 125.4 (qd,  $J_{\text{CF}} = 31.1$  Hz,  $J_{\text{CP}} = 3.6$  Hz), 123.6 (s), 30.4 (d,  $J_{\text{CP}} = 28.7$  Hz), 27.8 (s), 27.2 (d,  $J_{\text{CP}} = 10.0$  Hz), 26.2 (s);  $^{19}\text{F}$  NMR (376 MHz, DMSO- $d_6$ )  $\delta$  –69.6 (d,  $J = 2.8$  Hz);  $^{31}\text{P}$  NMR (161 MHz, DMSO- $d_6$ )  $\delta$  16.2 (s); HRMS (ESI)  $m/z$  calcd. for  $\text{C}_{25}\text{H}_{39}\text{BF}_3\text{ClP}$   $[\text{M} + \text{Cl}]^-$  473.2529, found 473.2529.

**3.2.23. B-4-(Trifluoromethyl)phenyl Dicyclohexylphosphine–Borane (38)**

White solid; Yield 37%, 132 mg, MP 52.7–53.7 °C;  $^1\text{H}$  NMR (400 MHz, acetone- $d_6$ )  $\delta$  7.54 (d,  $J = 7.1$  Hz, 2H), 7.40 (d,  $J = 8.0$  Hz, 2H), 4.27 (d,  $J = 357.0$  Hz, 1H), 2.45–1.63 (br, 2H), 2.13–2.03 (m, 2H), 1.86–1.66 (m, 10H), 1.46–1.25 (m, 10H);  $^{11}\text{B}$  NMR (128 MHz, DMSO- $d_6$ )  $\delta$  –29.4 (s);  $^{13}\text{C}$  NMR (100 MHz, acetone- $d_6$ )  $\delta$  137.0 (d,  $J_{\text{CP}} = 7.7$  Hz), 126.9 (qd,  $J_{\text{CF}} = 31.4$  Hz,  $J_{\text{CP}} = 4.1$  Hz), 126.3 (qd,  $J_{\text{CF}} = 270.8$  Hz,  $J_{\text{CP}} = 1.3$  Hz), 124.3–124.2 (m), 30.1 (s), 29.8 (d,  $J_{\text{CP}} = 31.3$  Hz), 29.1 (s), 27.4 (d,  $J_{\text{CP}} = 10.4$  Hz), 27.2 (d,  $J_{\text{CP}} = 11.7$  Hz), 26.5 (d,  $J_{\text{CP}} = 1.1$  Hz);  $^{19}\text{F}$  NMR (376 MHz, DMSO- $d_6$ )  $\delta$  –60.7 (d,  $J_{\text{FP}} = 3.4$  Hz);  $^{31}\text{P}$  NMR (161 MHz, DMSO- $d_6$ )

$\delta$  10.5 (d,  $J = 368.2$  Hz); HRMS (ESI)  $m/z$  calcd. for  $C_{19}H_{29}BF_3NaP$   $[M + Na]^+$  379.1944, found 379.1964.

### 3.2.24. *B*-4-(Trifluoromethyl)phenyl Tris(dimethylamino)phosphine–Borane (39)

White solid; Yield:23%, 73 mg; MP 41.1–41.6 °C;  $^1H$  NMR (400 MHz, DMSO- $d_6$ )  $\delta$  7.48 (d,  $J = 7.1$  Hz, 2H), 7.39 (d,  $J = 8.1$  Hz, 2H), 2.53 (d,  $J = 9.1$  Hz, 18H), 2.30–1.56 (br, 2H);  $^{11}B$  NMR (128 MHz, DMSO- $d_6$ )  $\delta$  –27.2 (d,  $J = 102.7$  Hz);  $^{13}C$  NMR (125 MHz, DMSO- $d_6$ ):  $\delta$  136.8 (d,  $J_{CP} = 7.8$  Hz), 125.6 (q,  $J_{CF} = 271.7$  Hz), 125.3 (qd,  $J_{CF} = 31.2$  Hz,  $J_{CP} = 3.9$  Hz), 123.42–123.37 (m), 37.4 (d,  $J_{CP} = 3.3$  Hz);  $^{19}F$  NMR (376 MHz, DMSO- $d_6$ )  $\delta$  –60.6 (d,  $J = 3.9$  Hz);  $^{31}P$  NMR (161 MHz, DMSO- $d_6$ )  $\delta$  92.5 (s); HRMS (ESI)  $m/z$  calcd. for  $C_{13}H_{24}BF_3N_3KP$   $[M + K]^+$  360.1385, found 360.1398.

### 3.3. Determination of Hydrophobicity ( $LogP$ )

The 1-octanol/water partition coefficient  $P$  was determined using HPLC based on the OECD Guideline for Testing Chemicals. A COSMOSIL Packed Column 5C18-MS-II (5  $\mu$ m, 150 mm  $\times$  4.6 mm id, Nacalai Tesque, Inc., Kyoto, Japan) was fitted on an HPLC instrument (Multiwavelength Detector, MD-2010 Plus, JASCO, Tokyo, Japan) equipped with a pump (PU-2080, JASCO) and an oven (SSC-2120, Senshu Scientific Co., Ltd., Tokyo, Japan). The injection volume was 20  $\mu$ L; the mobile phase was methanol–water 75% ( $v/v$ ); and the flow rate was 1.0 mL/min in all cases. Compounds were detected by measuring the UV absorption at 240 nm. The temperature of the column was kept at 40.0 ( $\pm$  0.1) °C during the measurement. The measurement was performed in triplicate, and the mean value was calculated. The dead time  $t_0$  was measured with thiourea as the unretained compound, and the capacity factor  $k$  was calculated using the equation  $\log k = \log (t_r - t_0/t_0)$ , where  $t_r$  represents the retention time of the compound. A calibration graph was determined experimentally using reference compounds (4-methylphenol, 4-chlorophenol, 4-phenylphenol, diphenylether, fluoranthene, and dichlorodiphenyltrichloroethane) with known  $logP$  values. The  $LogP$  values of phosphine–boranes were calculated based on a calibration graph ( $LogP = 2.6269 \log k_w + 3.059$ ,  $R^2 = 0.9915$ ).

### 3.4. T47D Alkaline Phosphatase Assay for the Evaluation of PR Antagonistic Activity

T47D alkaline phosphatase assays were performed as previously described, with minor modifications [40]. Briefly, the human breast cancer cell line T47D (HMS LINCS database Accession Numbers: 50541) was routinely cultivated in RPMI 1640 medium with 10% FBS at 37 °C in a 5% CO<sub>2</sub> humidified incubator. The cells were plated in 96-well plates and incubated overnight in a 5% CO<sub>2</sub> humidified incubator at 37 °C. The next day, the cells were treated with a fresh medium containing the test compound in the presence of 1 nM of progesterone and further incubated for 48 h. The medium was aspirated, and the cells were fixed with 100  $\mu$ L of 1.8% formalin–PBS. The fixed cells were washed with PBS, and 100  $\mu$ L of an assay buffer (1 mg/mL *p*-nitrophenol phosphate in diethanolamine water solution, pH 9.0) was added. The mixture was incubated at room temperature for 2 h under light-shielded conditions. The absorbance was measured at 405 nm using a DTX 880 Multimode Detector (Beckman Coulter, Brea, CA, USA). All data points were measured in triplicate, and IC<sub>50</sub> values were calculated from three independent experiments.

### 3.5. PR LBD Competitive Binding Assay

PR binding affinity was assessed using a PolarScreen Progesterone Receptor Competitor Assay Kit, Green (Invitrogen, Waltham, MA, USA, A15905) based on the manufacturer's instruction. Briefly, PR-LBD(GST)/Fluormone PR Green Complex (final concentration: 6.5 nM) and test compounds (final concentration: 100 nM to 32  $\mu$ M for the phosphine–boranes and 1 nM–320 nM for P4) in the assay buffer (final volume: 32  $\mu$ M) were mixed on a 384-well plate (black, polypropylene). Then, the mixture was incubated at room temperature for 1 h under shade. The fluorescence polarization value (mP) was measured at 485 nm/535 nm (excitation/emission) on a DTX 880 Multimode Detector (Beckman Coulter).

### 3.6. Docking Simulation

The structure of the LBD of hPR was prepared from the Protein Data Bank accession number 3G8O [56]. Polar hydrogen atoms and partial atomic charges were assigned using AutoDockTools (ADT). Molecular docking was performed using AutoDock 4.2 with the genetic algorithm. The AutoDock parameters for boron atoms were  $R_{ii} = 4.08$  and  $e_{ii} = 0.180$ .

## 4. Conclusions

To expand the utility of phosphine–boranes in medicinal chemistry, we designed and synthesized a series of *B*-(trifluoromethyl)phenyl phosphine–borane derivatives and investigated their hydrophobic characteristics and biological activity toward the PR. The synthesized *B*-(trifluoromethyl)phenyl phosphine–borane derivatives exhibited predictable  $\text{Log}P$  values. We also demonstrated that the P–H group in phosphine–borane was nonpolar. Biological evaluation revealed that all synthesized phosphine–boranes, except for the secondary phosphine derivatives, exhibited PR antagonistic activity. The potency of the compounds depended on the bulkiness of the phosphine moiety, and the tricyclopropylphosphine substructure was found to be the most suitable for the designed PR antagonists. Docking simulations suggested that the tricyclopropylphosphine moiety plays an important role in ligand–receptor interactions and that optimization of the phenyl moiety could lead to the development of novel PR antagonists with improved potency. These results support the idea that phosphine–boranes are versatile structural options in medicinal chemistry for a wide variety of drug candidates, and the developed compounds, including **22** and **34**, are promising lead compounds for further structural development of next-generation PR antagonists.

**Supplementary Materials:** The following supporting information can be downloaded at: <https://www.mdpi.com/article/10.3390/molecules29071587/s1>,  $^1\text{H}$ ,  $^{13}\text{C}$ ,  $^{11}\text{B}$ ,  $^{19}\text{F}$  and  $^{31}\text{P}$  NMR Spectra of synthesized compounds.

**Author Contributions:** Conceptualization, S.F.; formal analysis, Y.M., funding acquisition, S.F. investigation, Y.M., K.O. and S.F.; project administration, S.F.; writing—original draft preparation, Y.M.; writing—review and editing, S.F. All authors have read and agreed to the published version of the manuscript.

**Funding:** This work was partially supported by Grants-in-Aid for Scientific Research from JSPS (KAKENHI Grant Nos. 23K06046 (S.F.)), the Takeda Science Foundation (S.F.), the Hoansha Foundation (S.F.), and the Research Center for Biomedical Engineering (S.F.). This research was also partially supported by AMED under Grant Number JP23ama121043 (Research Support Project for Life Science and Drug Discovery, BINDS).

**Institutional Review Board Statement:** Not applicable.

**Informed Consent Statement:** Not applicable.

**Data Availability Statement:** The data are contained within the article and Supplementary Materials.

**Acknowledgments:** We thank Yosuke Demizu for kind assistance with the PR competitive binding assay.

**Conflicts of Interest:** The authors declare no conflicts of interest.

## References

1. Staubitz, A.; Robertson, A.P.; Sloan, M.E.; Manners, I. Amine– and phosphine– borane adducts: New interest in old molecules. *Chem. Rev.* **2010**, *110*, 4023–4078. [[CrossRef](#)]
2. Brunel, J.M.; Faure, B.; Maffei, M. Phosphane-boranes: Synthesis, characterization and synthetic applications. *Coord. Chem. Rev.* **1998**, *178*, 665–698. [[CrossRef](#)]
3. Paine, R.T.; Noth, H. Recent advances in phosphinoborane chemistry. *Chem. Rev.* **1995**, *95*, 343–379. [[CrossRef](#)]
4. Imamoto, T.; Kusumoto, T.; Suzuki, N.; Sato, K. Phosphine oxides and  $\text{LiAlH}_4$ – $\text{NaBH}_4$ – $\text{CeCl}_3$ ; synthesis and reactions of phosphine-boranes. *J. Am. Chem. Soc.* **1985**, *107*, 5301–5302. [[CrossRef](#)]
5. Imamoto, T.; Oshiki, T. Synthesis of Organic phosphorus compounds containing a linear P–B bond chain. *Tetrahedron Lett.* **1989**, *30*, 383–384. [[CrossRef](#)]
6. Imamoto, T.; Oshiki, T.; Onozawa, T.; Kusumoto, T.; Sato, K. Synthesis and reactions of phosphine–boranes. Synthesis of new bidentate ligands with homochiral phosphine centers via optically pure phosphine–boranes. *J. Am. Chem. Soc.* **1990**, *112*, 5244–5252. [[CrossRef](#)]

7. Li, P.; Sergueeva, Z.A.; Dobrikov, M.; Shaw, B.R. Nucleoside and oligonucleoside boranophosphates: Chemistry and properties. *Chem. Rev.* **2007**, *107*, 4746–4796. [[CrossRef](#)]
8. Summers, J.S.; Shaw, B. Boranophosphates as mimics of natural phosphodiesterases in DNA. *Curr. Med. Chem.* **2001**, *8*, 1147–1155. [[CrossRef](#)] [[PubMed](#)]
9. Schlieve, C.R.; Tam, A.; Nilsson, B.L.; Lieven, C.J.; Raines, R.T.; Levin, L.A. Synthesis and characterization of a novel class of reducing agents that are highly neuroprotective for retinal ganglion cells. *Exp. Eye Res.* **2006**, *83*, 1252–1259. [[CrossRef](#)]
10. Remtulla, R.; Das, S.K.; Levin, L.A. Predicting absorption-distribution properties of neuroprotective phosphine-borane compounds using in silico modeling and machine learning. *Molecules* **2021**, *26*, 2505. [[CrossRef](#)]
11. Saito, H.; Matsumoto, Y.; Hashimoto, Y.; Fujii, S. Phosphine boranes as less hydrophobic building blocks than alkanes and silanes: Structure-property relationship and estrogen-receptor-modulating potency of 4-phosphinophenol derivatives. *Bioorg. Med. Chem.* **2020**, *28*, 115310. [[CrossRef](#)]
12. Miyajima, Y.; Noguchi-Yachide, T.; Ochiai, K.; Fujii, S. Physicochemical characterization of B-hydroxyphenyl phosphine borane derivatives and their evaluation as nuclear estrogen receptor ligands. *RSC Med. Chem.* **2024**, *15*, 119–126. [[CrossRef](#)] [[PubMed](#)]
13. Mangelsdorf, D.J.; Thummel, C.; Beato, M.; Herrlich, P.; Schütz, G.; Umesono, K.; Blumberg, B.; Kastner, P.; Mark, M.; Chambon, P.; et al. The nuclear receptor superfamily: The second decade. *Cell* **1995**, *83*, 835–839. [[CrossRef](#)]
14. Aupperlee, M.D.; Smith, K.T.; Kariagina, A.; Haslam, S.Z. Progesterone receptor isoforms A and B: Temporal and spatial differences in expression during murine mammary gland development. *Endocrinology* **2005**, *146*, 3577–3588. [[CrossRef](#)]
15. Kolatorova, L.; Vitku, J.; Suchopar, J.; Hill, M.; Parizek, A. Progesterone: A steroid with wide range of effects in physiology as well as human medicine. *Int. J. Mol. Sci.* **2022**, *23*, 7989. [[CrossRef](#)]
16. Africander, D.; Verhoog, N.; Hapgood, J.P. Molecular mechanisms of steroid receptor-mediated actions by synthetic progestins used in HRT and contraception. *Steroids* **2011**, *76*, 636–652. [[CrossRef](#)] [[PubMed](#)]
17. Spitz, I.M. Progesterone antagonists and progesterone receptor modulators: An overview. *Steroids* **2003**, *68*, 981–993. [[CrossRef](#)]
18. Islam, M.S.; Afrin, S.; Jones, S.I.; Segars, J. Selective progesterone receptor modulators-mechanisms and therapeutic utility. *Endocr. Rev.* **2020**, *41*, bnaa012. [[CrossRef](#)] [[PubMed](#)]
19. Critchley, H.O.D.; Chodankar, R.R. Selective progesterone receptor modulators in gynaecological therapies. *J. Mol. Endocrinol.* **2020**, *65*, T15–T33. [[CrossRef](#)]
20. Singh, S.S.; Belland, L. Contemporary management of uterine fibroids: Focus on emerging medical treatments. *Curr. Med. Res. Opin.* **2015**, *31*, 1–12. [[CrossRef](#)]
21. Proietti, C.J.; Cenciarini, M.E.; Elizalde, P.V. Revisiting progesterone receptor (PR) actions in breast cancer: Insights into PR repressive functions. *Steroids* **2018**, *133*, 75–81. [[CrossRef](#)] [[PubMed](#)]
22. Soria, V.; Gonzalez-Rodriguez, A.; Huerta-Ramos, E.; Usall, J.; Cobo, J.; Bioque, M.; Barbero, J.D.; Garcia-Rizo, C.; Tost, M.; Monreal, J.A.; et al. Targeting hypothalamic-pituitary-adrenal axis hormones and sex steroids for improving cognition in major mood disorders and schizophrenia: A systematic review and narrative synthesis. *Psychoneuroendocrinology* **2018**, *93*, 8–19. [[CrossRef](#)] [[PubMed](#)]
23. Brisken, C. Progesterone signalling in breast cancer: A neglected hormone coming into the limelight. *Nat. Rev. Cancer* **2013**, *13*, 385–396. [[CrossRef](#)]
24. Kim, J.J.; Kurita, T.; Bulun, S.E. Progesterone action in endometrial cancer, endometriosis, uterine fibroids, and breast cancer. *Endocr. Rev.* **2013**, *34*, 130–162. [[CrossRef](#)]
25. Goyeneche, A.A.; Carón, R.W.; Telleria, C.M. Mifepristone inhibits ovarian cancer cell growth in vitro and in vivo. *Clin. Cancer Res.* **2007**, *13*, 3370–3379. [[CrossRef](#)] [[PubMed](#)]
26. Liu, R.; Shi, P.; Nie, Z.; Liang, H.; Zhou, Z.; Chen, W.; Chen, H.; Dong, C.; Yang, R.; Liu, S.; et al. Mifepristone suppresses basal triple-negative breast cancer stem cells by down-regulating KLF5 expression. *Theranostics* **2016**, *6*, 533–544. [[CrossRef](#)] [[PubMed](#)]
27. Lee, O.; Choi, M.R.; Christov, K.; Ivancic, D.; Khan, S.A. Progesterone receptor antagonism inhibits progesterone-related carcinogenesis and suppresses tumor cell proliferation. *Cancer Lett.* **2016**, *376*, 310–317.
28. Sitruk-Ware, R. Reprint of pharmacological profile of progestins. *Maturitas* **2008**, *61*, 151–157. [[CrossRef](#)] [[PubMed](#)]
29. Moguilewsky, M.; Philibert, D. RU 38486: Potent antiglucocorticoid activity correlated with strong binding to the cytosolic glucocorticoid receptor followed by an impaired activation. *J. Steroid Biochem.* **1984**, *20*, 271–276. [[CrossRef](#)] [[PubMed](#)]
30. Jeng, M.H.; Langan-Fahey, S.M.; Jordan, V.C. Estrogenic actions of RU486 in hormone-responsive MCF-7 human breast cancer cells. *Endocrinology* **1993**, *6*, 2622–2630. [[CrossRef](#)]
31. Winneker, R.C.; Fensome, A.; Zhang, P.; Yudit, M.R.; McComas, C.C.; Unwalla, R.J. A new generation of progesterone receptor modulators. *Steroids* **2008**, *73*, 689–701. [[CrossRef](#)]
32. Zhang, P.; Terefenko, E.A.; Fensome, A.; Wrobel, J.; Winneker, R.; Lundeen, S.; Marschke, K.B.; Zhang, Z. 6-Aryl-1,4-dihydrobenzo[d][1,3]oxazin-2-ones: A novel class of potent, selective, and orally active nonsteroidal progesterone receptor antagonists. *J. Med. Chem.* **2002**, *45*, 4379–4382. [[CrossRef](#)]
33. Fensome, A.; Adams, W.R.; Adams, A.L.; Berrodin, T.J.; Cohen, J.; Huselton, C.; Illenberger, A.; Kern, J.C.; Hudak, V.A.; Marella, M.A.; et al. Design, synthesis, and SAR of new pyrrole-oxindole progesterone receptor modulators leading to 5-(7-fluoro-3,3-dimethyl-2-oxo-2,3-dihydro-1H-indol-5-yl)-1-methyl-1H-pyrrole-2-carbonitrile (WAY-255348). *J. Med. Chem.* **2008**, *51*, 1861–1873. [[CrossRef](#)]

34. Sakai, H.; Hirano, T.; Mori, S.; Fujii, S.; Masuno, H.; Kinoshita, M.; Kagechika, H.; Tanatani, A. 6-Arylcoumarins as novel nonsteroidal type progesterone antagonists: An example with receptor-binding-dependent fluorescence. *J. Med. Chem.* **2011**, *54*, 7055–7065. [CrossRef]
35. Fujii, S.; Yamada, A.; Nakano, E.; Takeuchi, Y.; Mori, S.; Masuno, H.; Kagechika, H. Design and synthesis of nonsteroidal progesterone receptor antagonists based on C,C'-diphenylcarborane scaffold as a hydrophobic pharmacophore. *Eur. J. Med. Chem.* **2014**, *84*, 264–277. [CrossRef]
36. Fujii, S.; Nakano, E.; Yanagida, N.; Mori, S.; Masuno, H.; Kagechika, H. Development of p-carborane-based nonsteroidal progesterone receptor antagonists. *Bioorg. Med. Chem.* **2014**, *22*, 5329–5337. [CrossRef]
37. Mori, S.; Takeuchi, Y.; Tanatani, A.; Kagechika, H.; Fujii, S. Development of 1, 3-diphenyladamantane derivatives as nonsteroidal progesterone receptor antagonists. *Bioorg. Med. Chem.* **2015**, *23*, 803–809. [CrossRef]
38. Fensome, A.; Bender, R.; Chopra, R.; Cohen, J.; Collins, M.A.; Hudak, V.; Malakian, K.; Lockhead, S.; Olland, A.; Svenson, K.; et al. Synthesis and structure-activity relationship of novel 6-aryl-1,4-dihydrobenzo[d]-[1,3]oxazine-2-thiones as progesterone receptor modulators leading to the potent and selective nonsteroidal progesterone receptor agonist tanaproget. *J. Med. Chem.* **2005**, *48*, 5092–5095. [CrossRef]
39. Collins, M.A.; Hudak, V.; Bender, R.; Fensome, A.; Zhang, P.; Miller, L.; Winneker, R.C.; Zhang, Z.; Zhu, Y.; Cohen, J.; et al. Novel pyrrole-containing progesterone receptor modulators. *Bioorg. Med. Chem. Lett.* **2004**, *14*, 2185–2189. [CrossRef]
40. Yamada, A.; Kazui, Y.; Yoshioka, H.; Tanatani, A.; Mori, S.; Kagechika, H.; Fujii, S. Development of N-(4-phenoxyphenyl) benzenesulfonamide derivatives as novel nonsteroidal progesterone receptor antagonists. *ACS Med. Chem. Lett.* **2016**, *7*, 1028–1033. [CrossRef]
41. Nishiyama, Y.; Mori, S.; Makishima, M.; Fujii, S.; Kagechika, H.; Hashimoto, Y.; Ishikawa, M. Novel nonsteroidal progesterone receptor (PR) antagonists with a phenanthridinone skeleton. *ACS Med. Chem. Lett.* **2018**, *9*, 641–645. [CrossRef] [PubMed]
42. Baban, J.A.; Roberts, B.P. Homolytic reactions of ligated boranes. Part 9. Overall addition of alkanes to electron-deficient alkenes by a radical chain mechanism. *J. Chem. Soc. Perkin Trans.* **1988**, *7*, 1195–1200. [CrossRef]
43. Kawano, Y.; Yamaguchi, K.; Miyake, S.Y.; Kakizawa, T.; Shimoi, M. Investigation of the stability of the M-H-B bond in borane  $\sigma$  complexes  $[M(CO)_5(\eta^1-BH_2R-L)]$  and  $[CpMn(CO)_2(\eta^1-BH_2R-L)]$  (M= Cr, W; L= tertiary amine or phosphine): Substituent and Lewis base effects. *Chem. Eur. J.* **2007**, *13*, 6920–6931. [CrossRef] [PubMed]
44. Leo, A.; Hansch, C.; Elkins, D. Partition coefficients and their uses. *Chem. Rev.* **1971**, *71*, 525–616. [CrossRef]
45. OECD. *Guideline for Testing of Chemicals 117, Partition Coefficient (n-octanol/Water), High Performance Liquid Chromatography (HPLC) Method*; OECD Publishing: Paris, France, 2022.
46. Finizio, A.; Vighi, M.; Sandroni, D. Determination of n-octanol/water partition coefficient ( $K_{ow}$ ) of pesticide critical review and comparison of methods. *Chemosphere* **1997**, *34*, 131–161. [CrossRef]
47. Hansch, C.; Leo, A.; Hoekman, D. *Exploring QSAR: Hydrophobic, Electronic, and Steric Constants*; American Chemical Society: Washington, DC, USA, 1995; Volume 2, ISBN 978-084-122-991-4.
48. Daina, A.; Michielin, O.; Zoete, V. SwissADME: A free web tool to evaluate pharmacokinetics, drug-likeness and medicinal chemistry friendliness of small molecules. *Sci. Rep.* **2017**, *7*, 42717. [CrossRef] [PubMed]
49. SwissADME. Available online: <http://www.swissadme.ch> (accessed on 27 September 2023).
50. Moriguchi, I.; Hirono, S.; Liu, Q.; Nakagome, I.; Matsushita, Y. Simple method of calculating octanol/water partition coefficient. *Chem. Pharm. Bull.* **1992**, *40*, 127–130. [CrossRef]
51. Moriguchi, I.; Hirono, S.; Nakagome, I.; Hirano, H. Comparison of reliability of log P values for drugs calculated by several methods. *Chem. Pharm. Bull.* **1994**, *42*, 976–978. [CrossRef]
52. Lipinski, C.A.; Lombardo, F.; Dominy, B.W.; Feeney, P.J. Experimental and computational approaches to estimate solubility and permeability in drug discovery and development settings. *Adv. Drug Deliv. Rev.* **1997**, *23*, 3–25. [CrossRef]
53. Lipinski, C.A. Lead-and drug-like compounds: The rule-of-five revolution. *Drug Discov. Today Technol.* **2004**, *1*, 337–341. [CrossRef]
54. Wildman, S.A.; Crippen, G.M. Prediction of physicochemical parameters by atomic contributions. *J. Chem. Inf. Comput. Sci.* **1999**, *39*, 868–873. [CrossRef]
55. Di Lorenzo, D.; Albertini, A.; Zava, D. Progesterone regulation of alkaline phosphatase in the human breast cancer cell line T47D. *Cancer Res.* **1991**, *51*, 4470–4475. [PubMed]
56. Hiraoka, D.; Nakamura, N.; Nishizawa, Y.; Uchida, N.; Noguchi, S.; Matsumoto, K.; Sato, B. Inhibitory and stimulatory effects of glucocorticoid on androgen-induced growth of murine Shionogi carcinoma 115 in vivo and in cell culture. *Cancer Res.* **1987**, *47*, 6560–6564. [PubMed]
57. Thompson, S.K.; Washburn, D.G.; Frazee, J.S.; Madauss, K.P.; Hoang, T.H.; Lapinski, L.; Grygielko, E.T.; Glace, L.E.; Trizna, W.; Williams, S.P.; et al. Rational design of orally-active, pyrrolidine-based progesterone receptor partial agonists. *Bioorg. Med. Chem. Lett.* **2009**, *19*, 4777–4780. [CrossRef]
58. Morris, G.M.; Huey, R.; Lindstrom, W.; Sanner, M.F.; Belew, R.K.; Goodsell, D.S.; Olson, A.J. AutoDock4 and AutoDockTools4: Automated docking with selective receptor flexibility. *J. Comput. Chem.* **2009**, *30*, 2785–2791. [CrossRef] [PubMed]

**Disclaimer/Publisher's Note:** The statements, opinions and data contained in all publications are solely those of the individual author(s) and contributor(s) and not of MDPI and/or the editor(s). MDPI and/or the editor(s) disclaim responsibility for any injury to people or property resulting from any ideas, methods, instructions or products referred to in the content.